Supplementary Material

Competition between phenothiazines and BH3 peptide for the binding site of the antiapoptotic BCL-2 protein

Aline Lagoeiro do Carmo[a], Fernanda Bettanin[b], Michell de Oliveira Almeida[c], Simone Queiroz Pantaleão[a], Tiago Rodrigues[a], Paula Homem-de-Mello[a,*], Kathia Maria Honorio[a,b,*]

[a] Centro de Ciências Naturais e Humanas, Universidade Federal do ABC, Santo André, São Paulo, Brazil.

[b] Escola de Artes, Ciências e Humanidades, Universidade de São Paulo (USP), São Paulo, Brazil.

[c] Instituto de Química de São Carlos, Universidade de São Paulo (USP), São Carlos, São Paulo, Brazil.

*Corresponding author emails: paula.mello@ufabc.edu.br, kmhonorio@usp.br

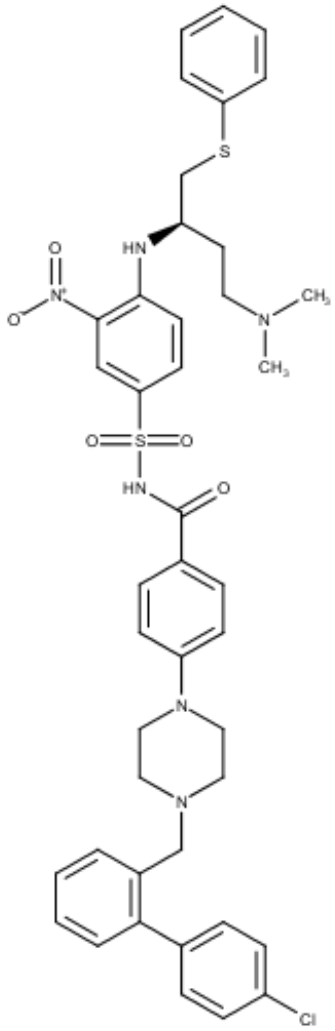

(a)

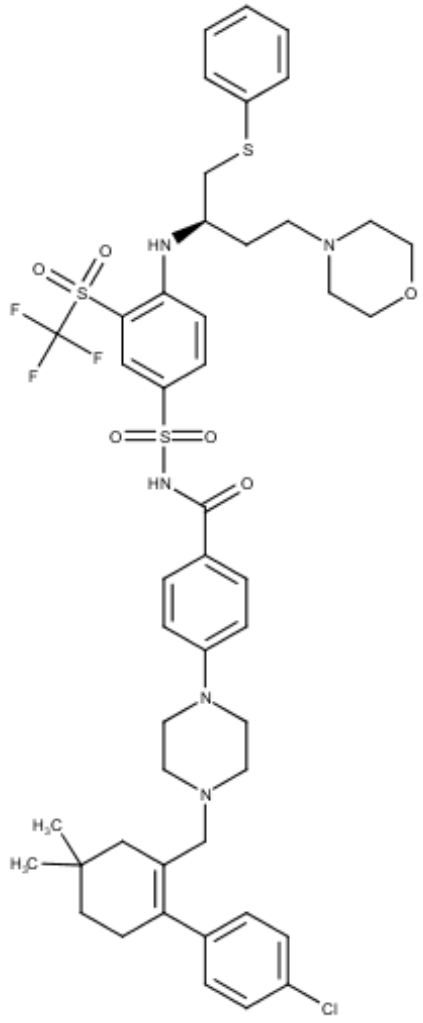

(b)

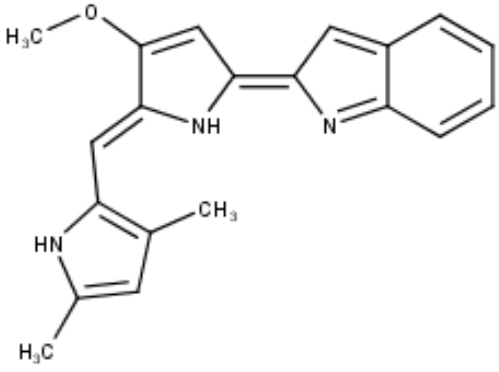

(c)

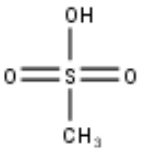

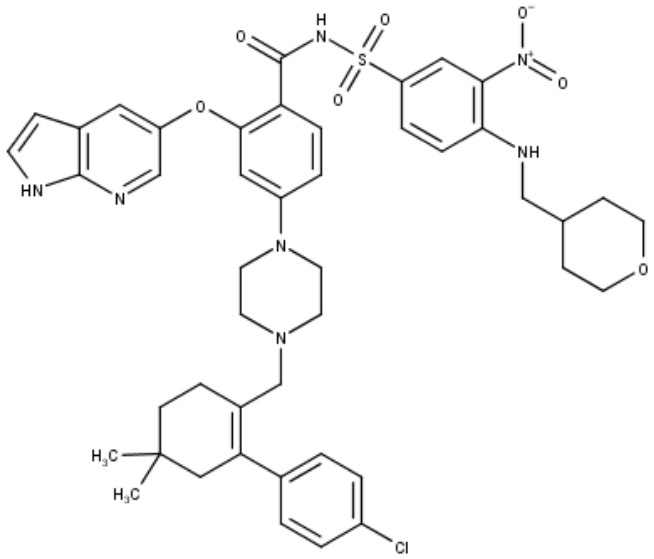

(d)

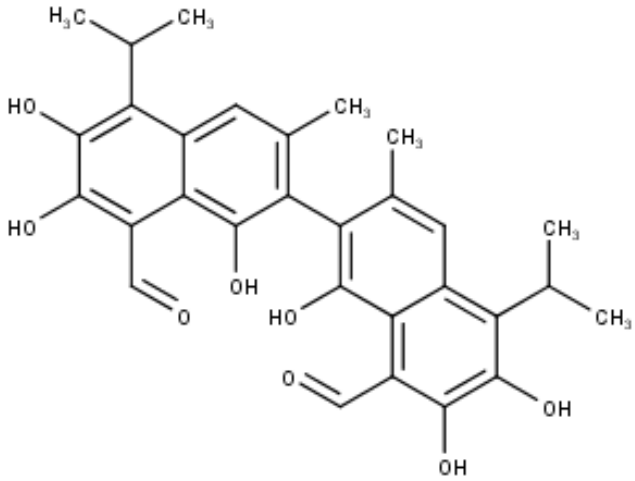

(e)

Figure S1. Structures of the compounds which are intended to mimic the BH3 domain that bind to the BH3 binding domain on BCL-2 antiapoptotic members: (a) ABT-737, (b) navitoclax (ABT-263), (c) obatoclax mesylate (GX15-070), (d) venetoclax (ABT-199) and (e) gossypol.

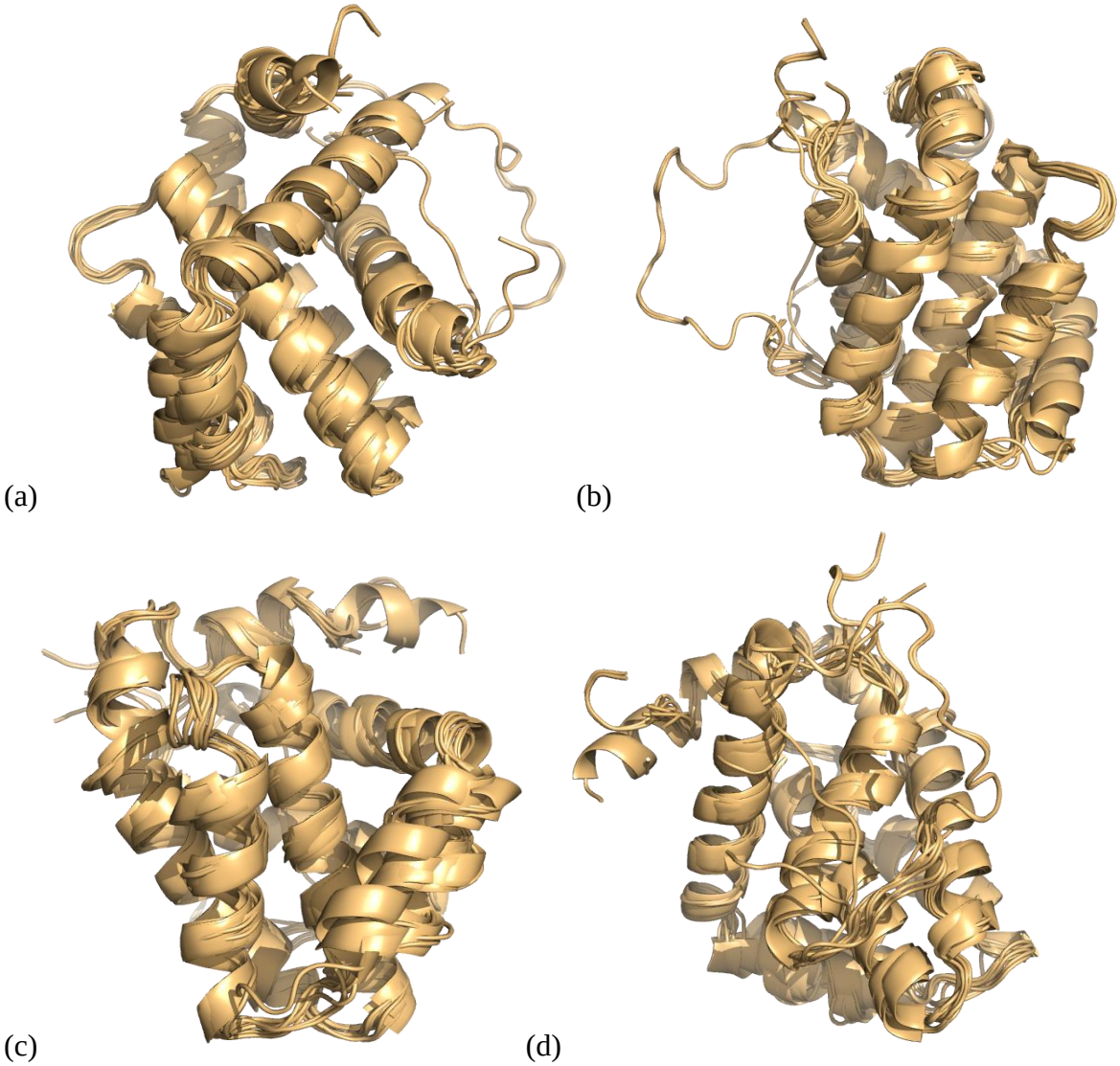

Figure S2. Alignment of human Bcl-2 protein A chain crystallographic structures (PDB_ID: 1YSW, 2O2F, 2O21, 2O22, 2W3L, 4AQ3, 4IEH, 4LVT, 4LXD, 4MAN, 5AGW, 5AGX, 5JSN): (a) left side view; (b) right side view, (c) front view and (d) rear view.

	1 (1YSW)	2 (2O2F)	3 (2O21)	4 (2O22)	5 (2W3L)	6 (4AQ3)	7 (4IEH)	8 (4LVT)	9 (4LXD)	10 (4MAN)	11 (5AGW)	12 (5AGX)	13 (5JSN)
1|	---	1.6	0.0	0.5	1.3	1.3	1.3	1.2	1.3	1.3	1.4	1.4	1.2
2|	1.6	---	1.6	1.6	1.6	1.5	1.4	1.4	1.4	1.4	1.6	1.6	1.7
3|	0.0	1.6	---	0.5	1.3	1.3	1.3	1.2	1.3	1.3	1.4	1.4	1.2
4|	0.5	1.6	0.5	---	1.4	1.3	1.3	1.2	1.3	1.3	1.4	1.5	1.3
5|	1.3	1.6	1.3	1.4	---	0.7	1.0	0.7	0.9	0.9	0.8	0.8	0.7
6|	1.3	1.5	1.3	1.3	0.7	---	0.8	0.9	0.7	0.8	0.8	0.9	0.8
7|	1.3	1.4	1.3	1.3	1.0	0.8	---	0.9	0.5	0.5	0.8	0.9	1.0
8|	1.2	1.4	1.2	1.2	0.7	0.9	0.9	---	0.8	0.8	0.9	1.1	0.9
9|	1.3	1.4	1.3	1.3	0.9	0.7	0.5	0.8	---	0.5	0.8	0.9	0.9
10|	1.3	1.4	1.3	1.3	0.9	0.8	0.5	0.8	0.5	---	0.9	0.9	1.0
11|	1.4	1.6	1.4	1.4	0.8	0.8	0.8	0.9	0.8	0.9	---	0.6	0.7
12|	1.4	1.6	1.4	1.5	0.8	0.9	0.9	1.1	0.9	0.9	0.6	---	0.9
13|	1.2	1.7	1.2	1.3	0.7	0.8	1.0	0.9	0.9	1.0	0.7	0.9	---

Figure S3. RMSD matrix of the alignment of the human Bcl-2 protein A chain crystallographic structures (PDB_ID: 1YSW, 2O2F, 2O21, 2O22, 2W3L, 4AQ3, 4IEH, 4LVT, 4LXD, 4MAN, 5AGW, 5AGX, 5JSN).

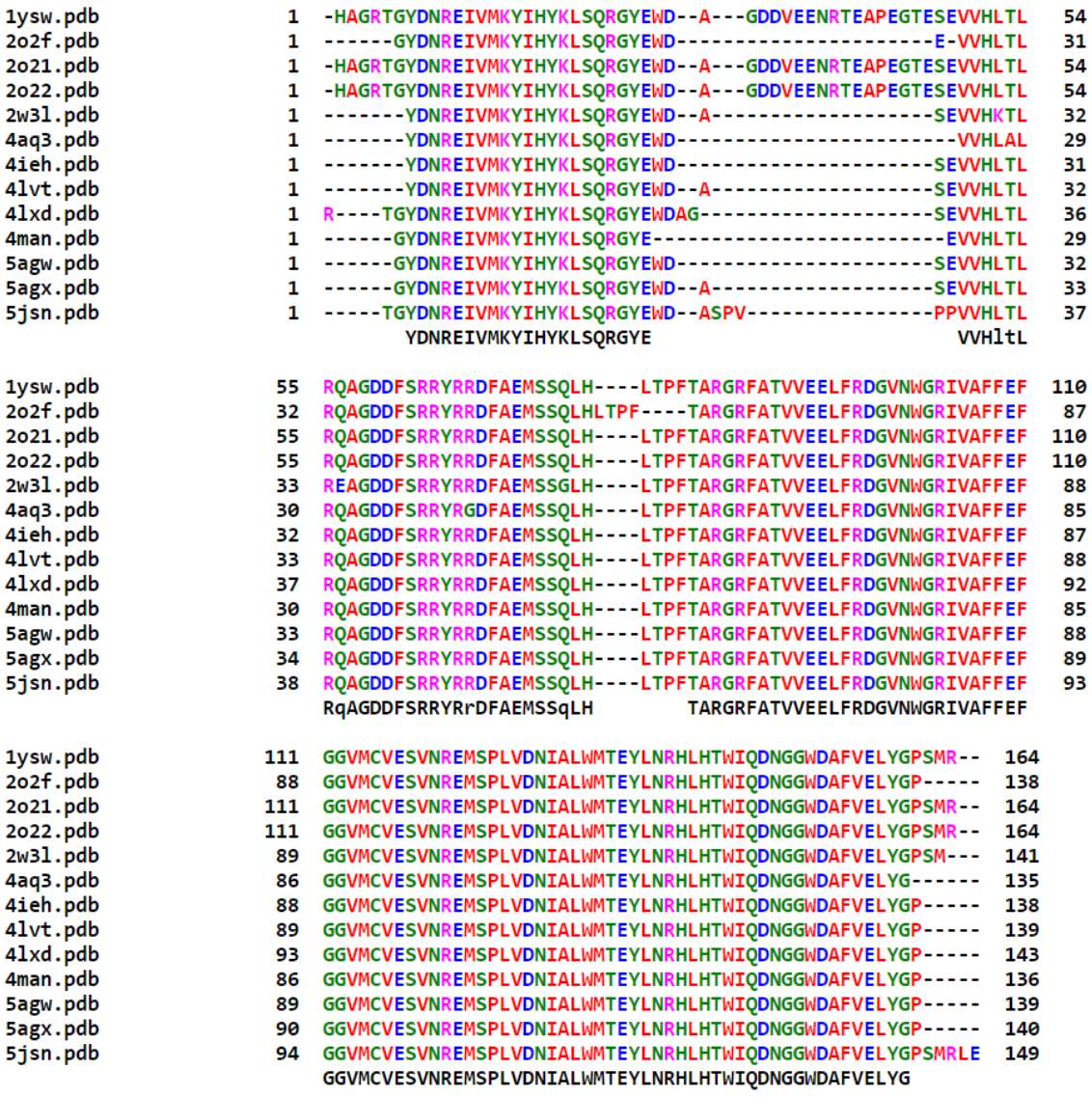

Figure S4. Alignment of A-chain crystallographic structures of human Bcl-2 protein (PDB_ID: 1YSW, 2O2F, 2O21, 2O22, 2W3L, 4AQ3, 4IEH, 4LVT, 4LXD, 4MAN, 5AGW, 5AGX, 5JSN), representing hydrophobic residues including aromatics (red), acids (blue), basic (pink) and basic with hydroxyl groups and / or amino groups (green); with the marking line below each stretch of the multiple alignment indicating fully conserved residues (upper case) and partially conserved residues (lower case).

Table S1. Characteristics of probes used by FTSite and FTMap servers

Probe	**Properties**[a]
Acetamide (ACD)	Polar, hydrogen bond acceptor and donor
Acetonitrile (ACN)	Polar and hydrogen bond acceptor character
Acetone (ACT)	Polar and hydrogen bond acceptor character
Acetaldehyde (ADY)	Polar and hydrogen bond acceptor character
Methylamine (AMN)	Polar, hydrogen bond acceptor and donor
Benzaldehyde (BDY)	Polar, aromatic and hydrogen bond acceptor character
Benzene (BEN)	Hydrophobic and aromatic
Butanol (BUT)	Polar and hydrogen bond acceptor character
Ciclohexane (CHX)	Polar, hydrogen bond acceptor and donor
N,N-dimethylformamide (DFO)	Polar and hydrogen bond acceptor character
Dimethyl ether (DME)	Polar and hydrogen bond acceptor character
Ethanol (EOL)	Polar, hydrogen bond acceptor and donor
Ethane (ETH)	Hydrophobic
Phenol (PHN)	Polar, aromatic, hydrogen bond acceptor and donor
Isopropanol (THS)	Polar and hydrogen bond acceptor character
Urea (URE)	Polar, hydrogen bond acceptor and donor

(a) (Bohnuud et al. 2012; Brenke et al. 2009; D. Kozakov et al. 2011; Dima Kozakov et al. 2015; Ngan et al. 2012)

Table S2. Hydrophobicity and hydrophilicity values by Kyte and Doolittle

Residues	**Kyte-Doolittle Values [a]**	**Classifications [b]**	**Color Scale [c]**
Ile	4.5	Hydrophobic	Orange-red
Val	4.2	Hydrophobic	Orange-red
Leu	3.8	Hydrophobic	Orange-red
Phe	2.8	Hydrophobic	Orange-red
Cys	2.5	Hydrophobic	Orange-red
Met	1.9	Hydrophobic	Orange-red
Ala	1.8	Hydrophobic	Orange-red
Gly	-0.4	Neutral	White
Thr	-0.7	Neutral	White
Ser	-0.8	Neutral	White
Trp	-0.9	Neutral	White
Tyr	-1.3	Neutral	White
Pro	-1.6	Neutral	White
His	-3.2	Hydrophilic	Blue
Glu	-3.5	Hydrophilic	Blue
Gln	-3.5	Hydrophilic	Blue
Asp	-3.5	Hydrophilic	Blue
Asn	-3.5	Hydrophilic	Blue
Lys	-3.9	Hydrophilic	Blue
Arg	-4.5	Hydrophilic	Blue

(a) Kyte and Doolittle, 1982.

(b) De Oliveira Rodrigues et al., 2015.

(c) Pettersen et al., 2004.

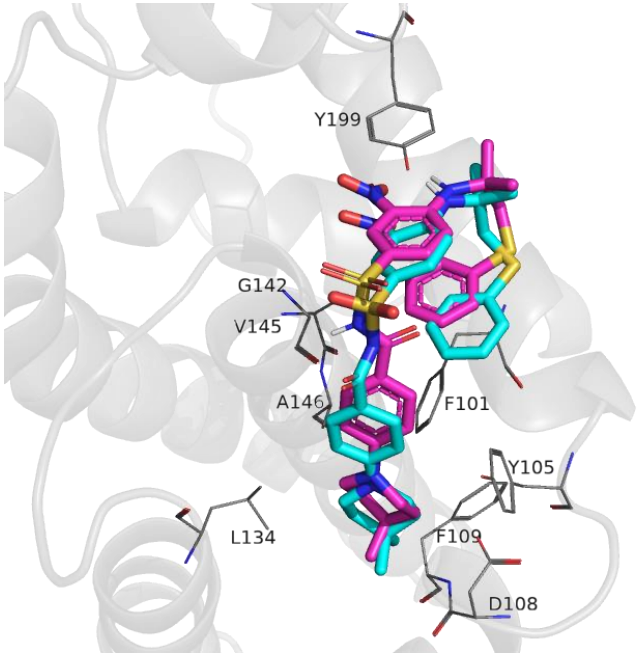

Figure S5. Representation of the molecular coupling of the ligand at the original position of the protein-ligand complex crystal structure (light pink) (PDB_ID: 2O22) and ligand overlap (Blue).

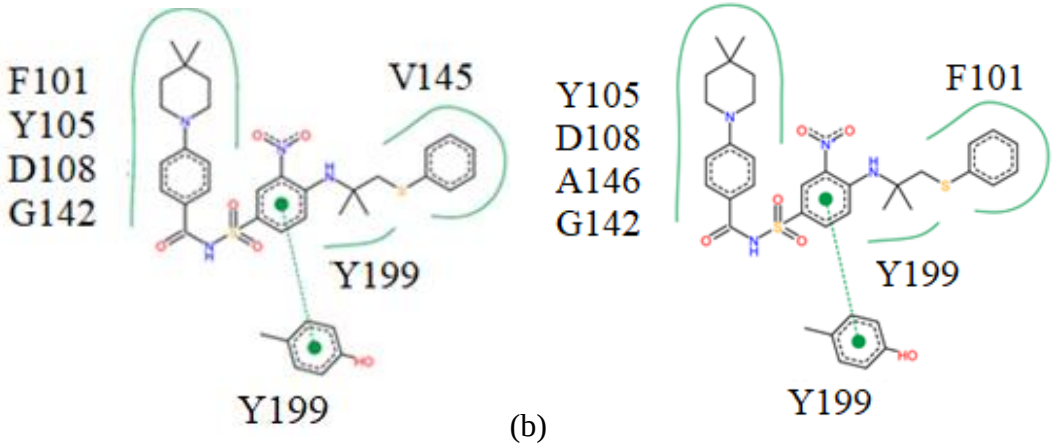

(a) (b)

Figure S6. Interactions Predicted by the Poseview Server. (a) crystallographic ligand pose (PDB_ID: 2O22) and (b) ligand pose obtained from re-coupling.

(a)

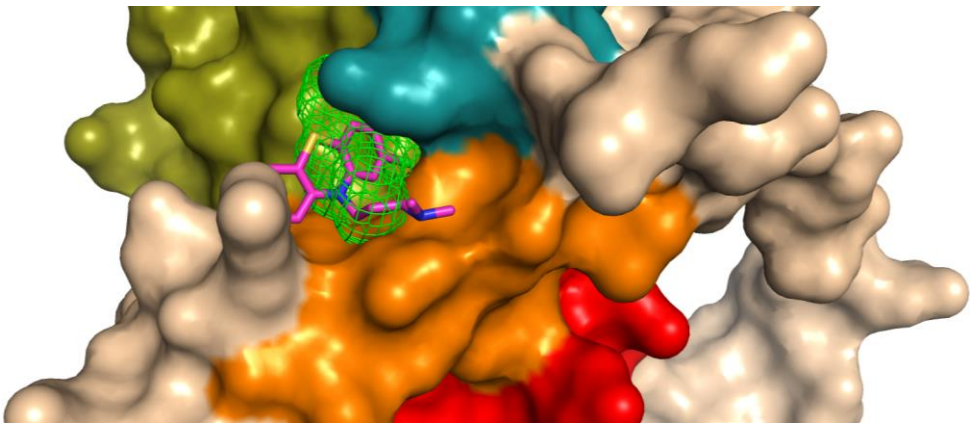

(b)

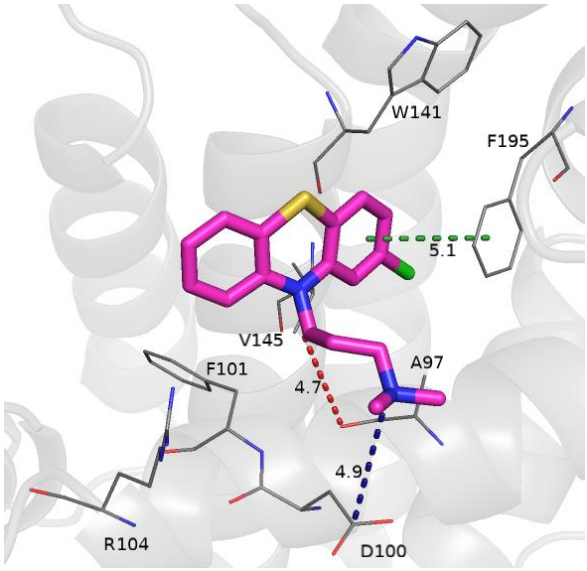

(c)

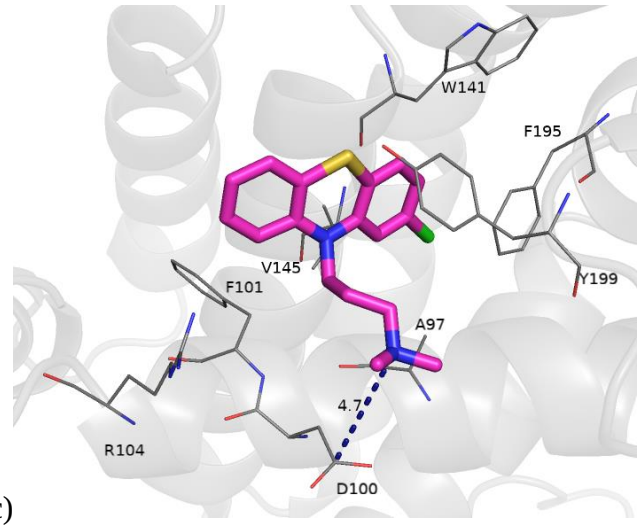

Figure S7. (a) Representation of BH1-BH4 domains (Figure 2) with presence of site 2 detected by FTSite server with aliphatic chlorpromazine subclass molecular coupling, (EC50 = (125.3 ± 1.1) μmol.L^{-1}) performed on the AutoDock Vina 1.5.7 program. Representation of the π-stacking (green), hydrogen bonding (red) and saline bridge (Blue) interaction of the molecular couplings performed in AutoDock Vina 1.5.7 (b) and Achilles Blind Docking (c) server, with additional interactions and / or confirmed by the BINANA 1.2.0 algorithm.

(a)

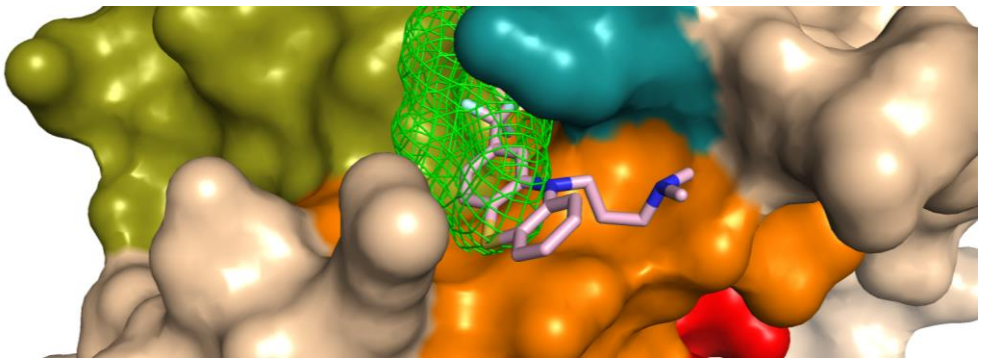

(b)

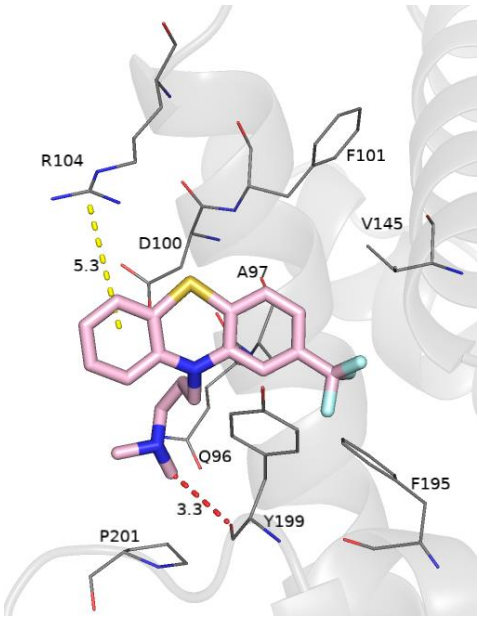

(c)

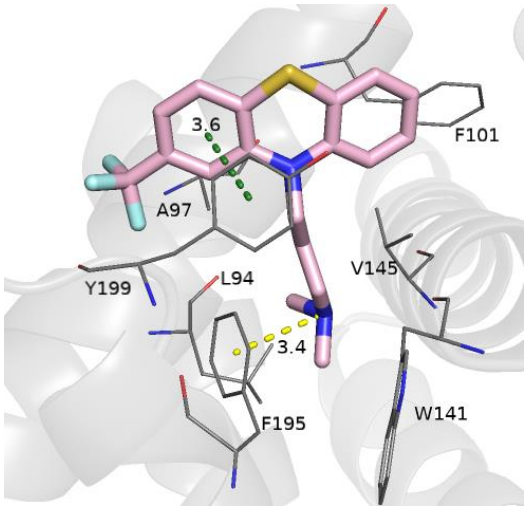

Figure S8. (a) Representation of BH1-BH4 domains (Figure 2) with the presence of site 2 detected by the FTSite server with the aliphatic subclass trifluprom azine molecular coupling (EC50 = (105.9 ± 1.0) μmol.L^{-1}) performed in the AutoDock Vina 1.5.7 program. Representation of π-stacking (green), cation-π (yellow) and hydrogen bonding (red) interactions of the molecular couplings performed in AutoDock Vina 1.5.7 (b) and Achilles Blind Docking (c) server, with interactions additional and / or confirmed by the BINANA 1.2.0 algorithm.

(a)

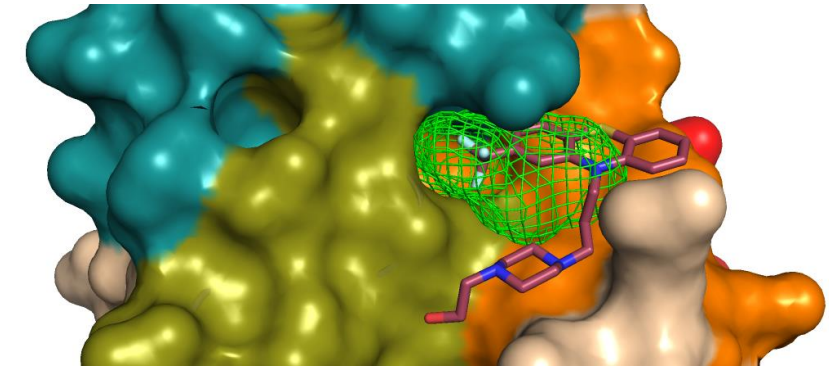

(b)

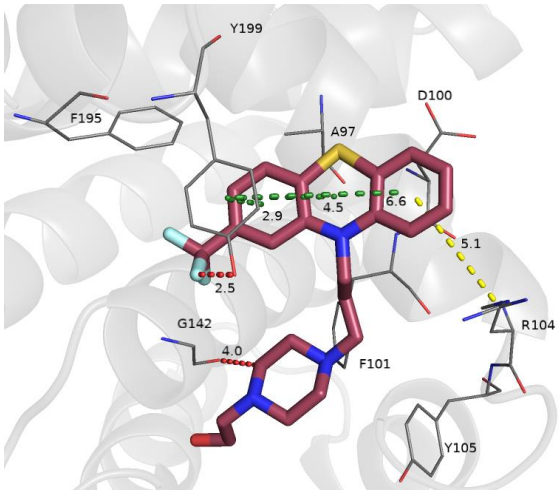

(c)

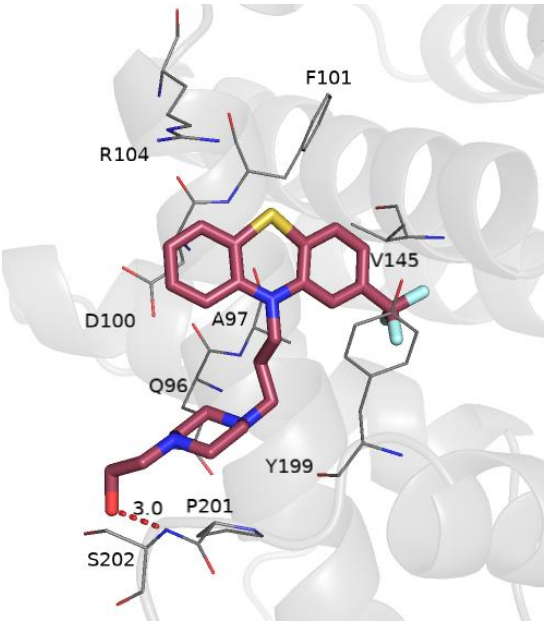

Figure S9. (a) Representation of BH1-BH4 domains (Figure 2) with presence of site 2 detected by FTSite server with piperazine subclass molecular coupling of fluphenazine (EC50 = (63.2 ± 1.0) μmol.L^{-1}) performed in the AutoDock Vina 1.5.7 program. Representation of π-stacking (green), cation-π (yellow) and hydrogen bonding (red) interactions of the molecular couplings performed in AutoDock Vina 1.5.7 (b) and Achilles Blind Docking (c) server, with interactions additional and / or confirmed by the BINANA 1.2.0 algorithm.

(a)

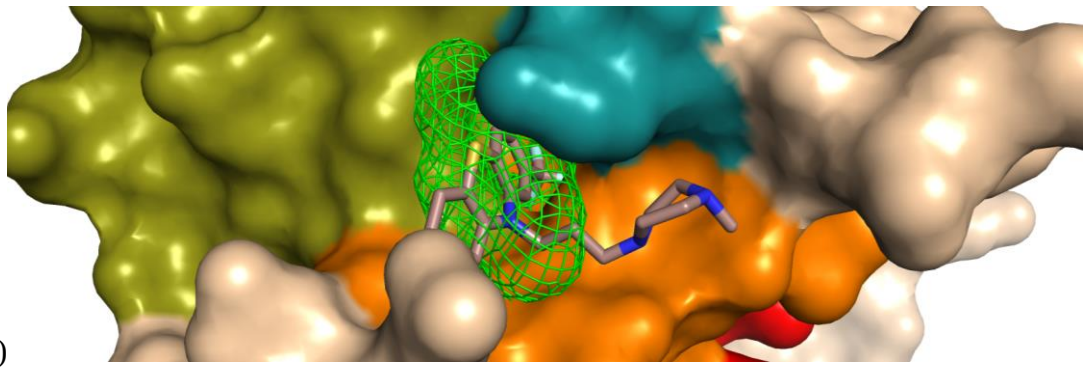

(b)

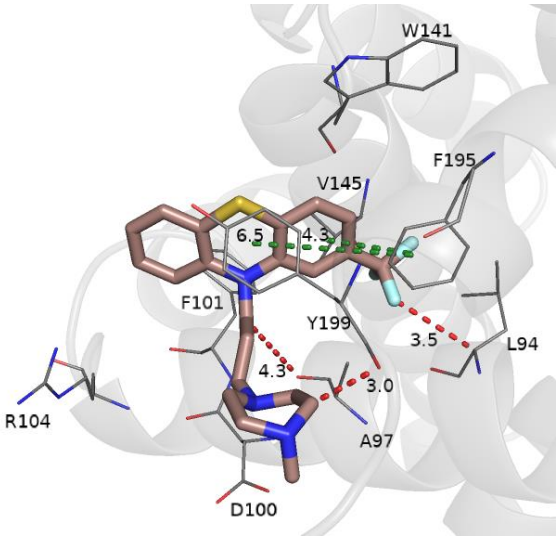

(c)

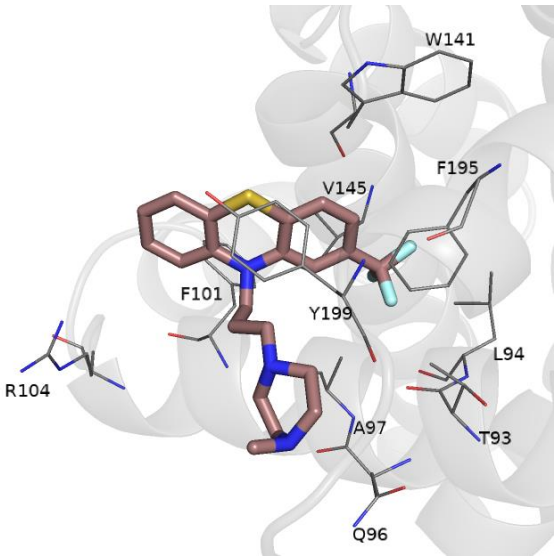

Figure S10. (a) Representation of BH1-BH4 domains (Figure 2) with the presence of site 2 detected by the FTSite server with the piperazine subclass trifluoperazine molecular coupling (EC50 = (56.2 ± 1.0) μmol.L^{-1}) performed in the AutoDock Vina 1.5.7 program. Representation of the π-stacking (green), hydrogen bonding (red) and saline bridge (Blue) interaction of the molecular couplings performed in AutoDock Vina 1.5.7 (b) and Achilles Blind Docking (c) server, with additional interactions and / or confirmed by the BINANA 1.2.0 algorithm.

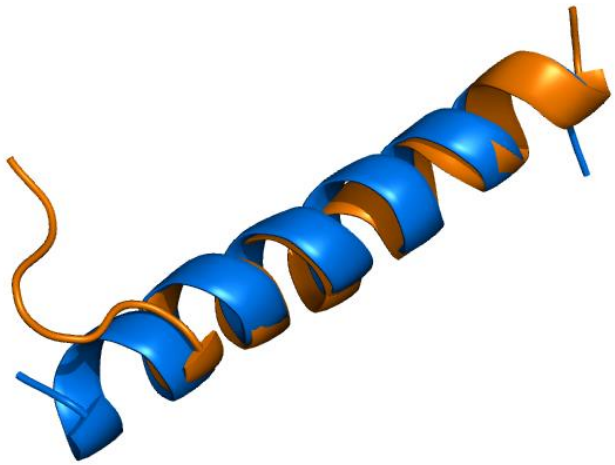

Figure S11. Representation of the molecular coupling of peptide BH3 in the original position of the crystalline structure (blue) (PDB_ID: 2XA0) in relation to the composition used by the coupling (orange) with the GalaxyPepDock server (RMSD 1.962 Å between the alpha helix amino acid residues).

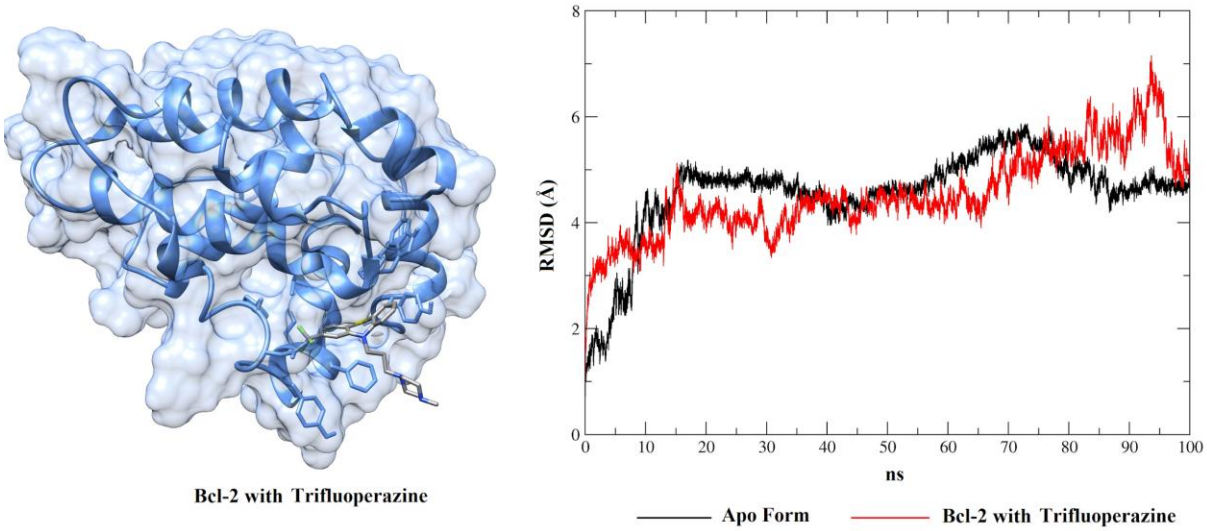

Figure S12. RMSD values of BCL-2 in Apo form (black), BCL-2 with trifluoperazine molecule (red) and 3D conformation obtained by clustering the MD.

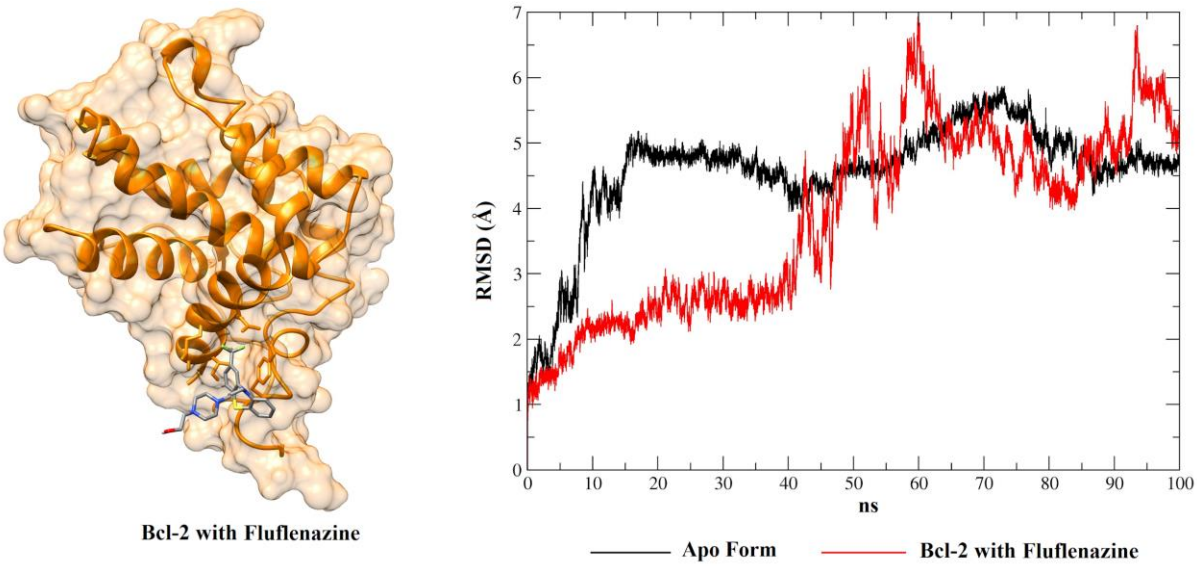

Figure S13. RMSD values of BCL-2 in Apo form (black), BCL-2 with fluphenazine molecule (red) and 3D conformation obtained by clustering the MD.

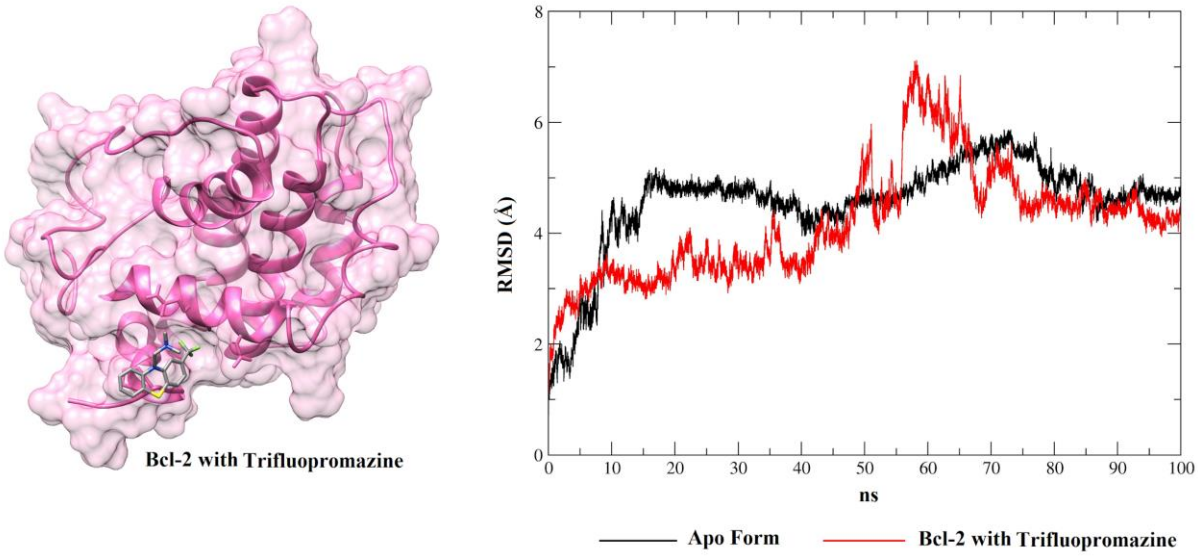

Figure S14. RMSD values of BCL-2 in Apo form (black), BCL-2 with trifluopromazine molecule (red) and 3D conformation obtained by clustering the MD.

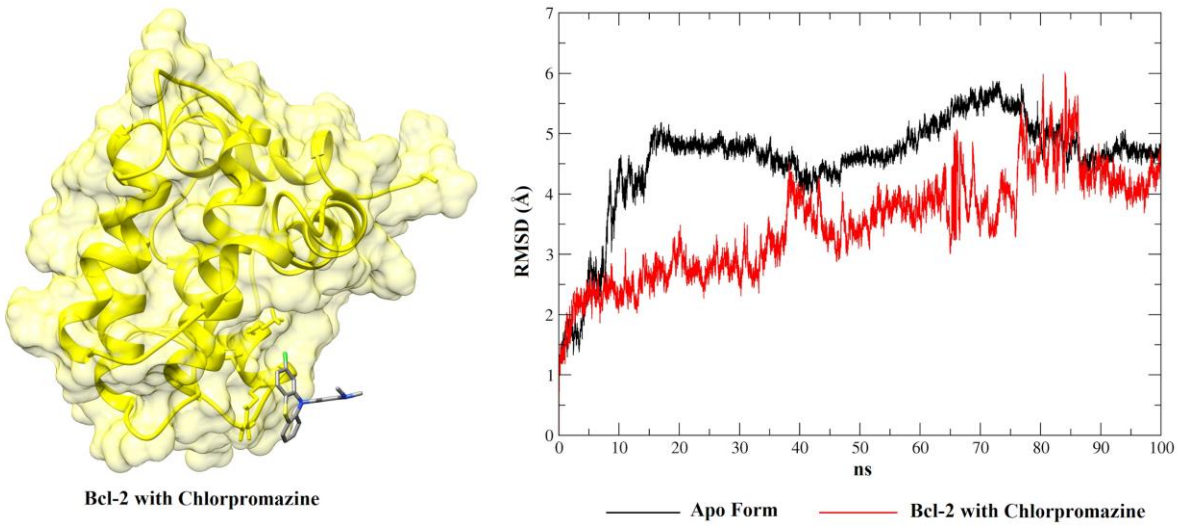

Figure S15. RMSD values of BCL-2 in Apo form (black), BCL-2 with chlorpromazine molecule (red) and 3D conformation obtained by clustering the MD.

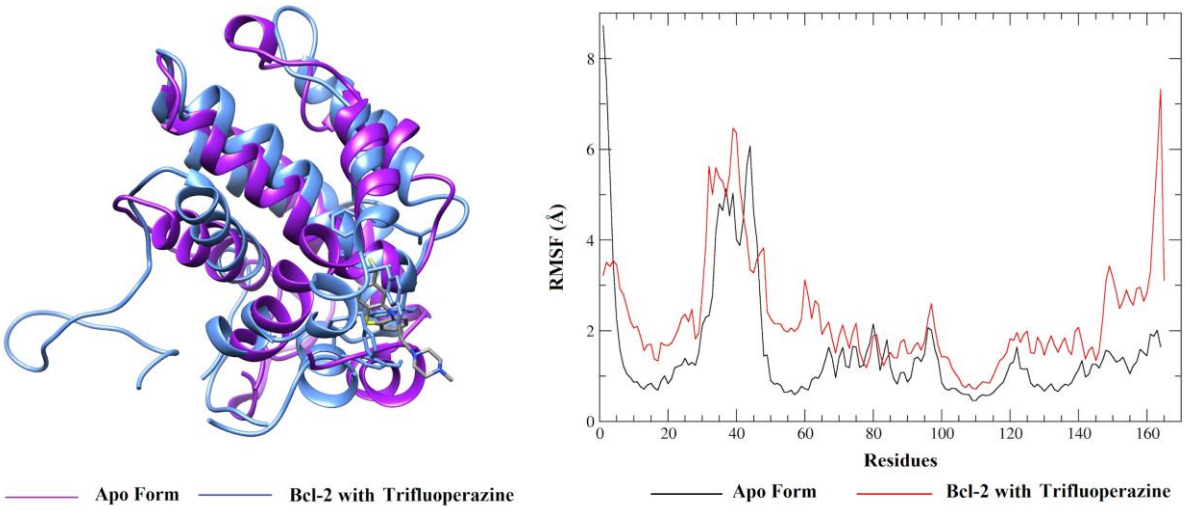

Figure S16. RMSF values of BCL-2 in the presence of trifluoperazine.

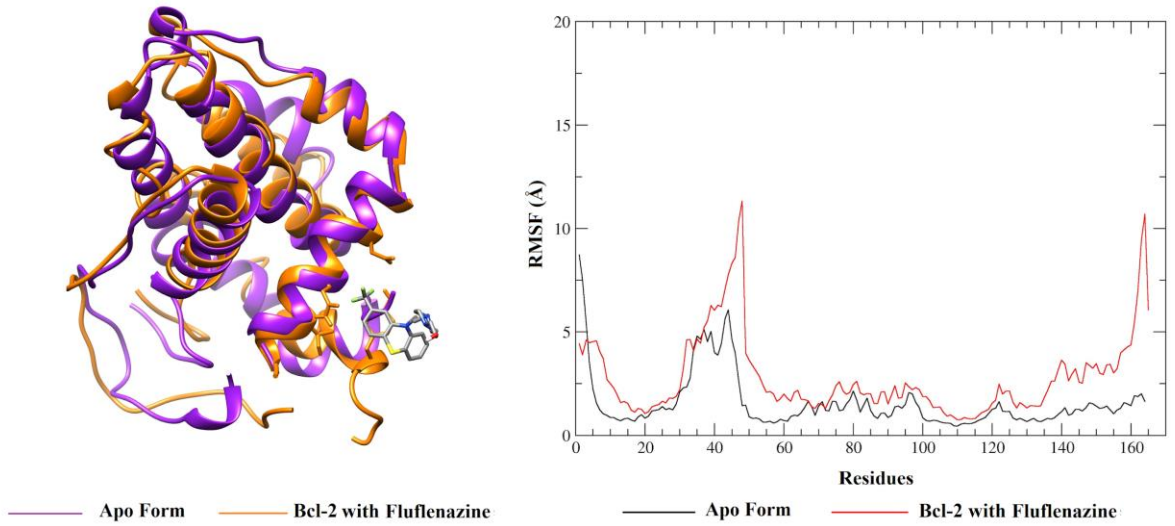

Figure S17. RMSF values of BCL-2 in the presence of fluphenazine.

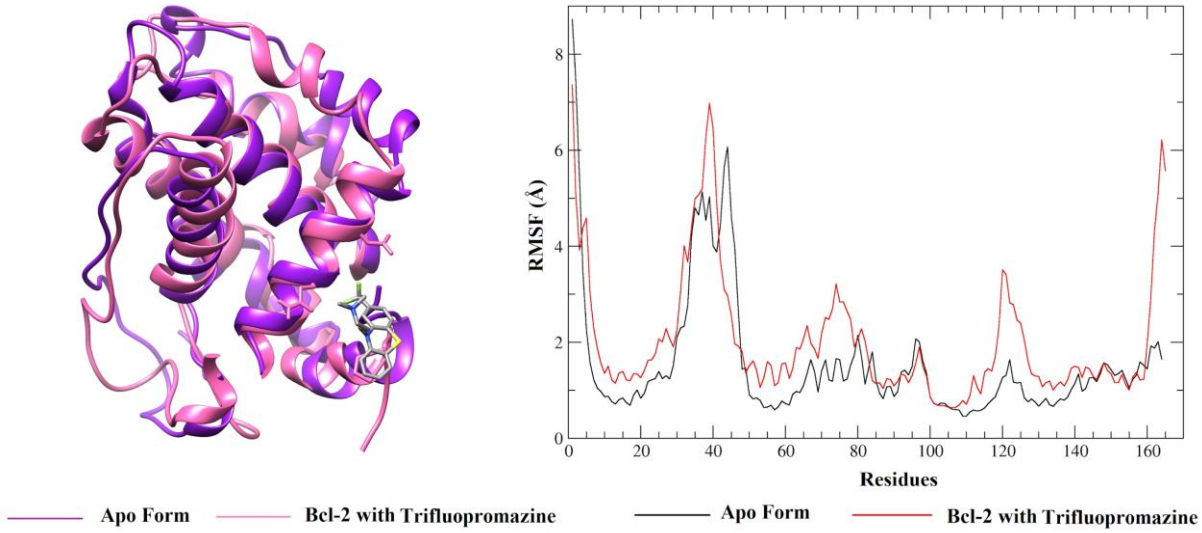

Figure S18. RMSF values of BCL-2 in the presence of triflupromazine.

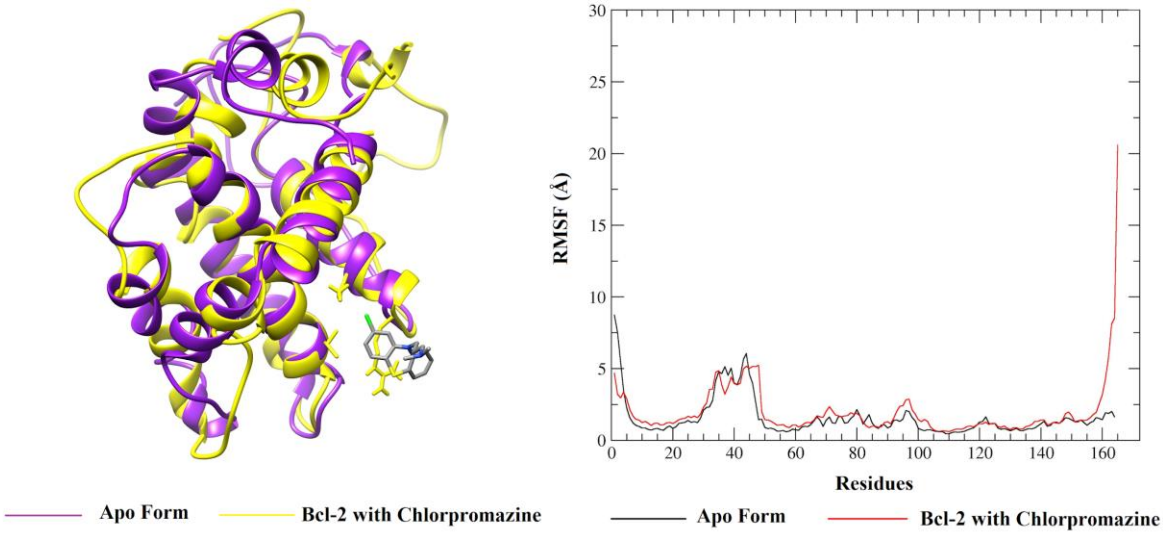

Figure S19. RMSF values of BCL-2 in the presence of chlorpromazine.

REFERENCES

Bohnuud, Tanggis et al. 2012. “Computational Mapping Reveals Dramatic Effect of Hoogsteen Breathing on Duplex DNA Reactivity with Formaldehyde.” *Nucleic Acids Research* 40(16): 7644–52. https://academic.oup.com/nar/article/40/16/7644/1032290.

Brenke, Ryan et al. 2009. “Fragment-Based Identification of Druggable ‘Hot Spots’ of Proteins Using Fourier Domain Correlation Techniques.” *Bioinformatics* 25(5): 621–27. https://academic.oup.com/bioinformatics/article-lookup/doi/10.1093/bioinformatics/btp036.

Kozakov, D. et al. 2011. “Structural Conservation of Druggable Hot Spots in Protein-Protein Interfaces.” *Proceedings of the National Academy of Sciences* 108(33): 13528–33. http://www.pnas.org/cgi/doi/10.1073/pnas.1101835108.

Kozakov, Dima et al. 2015. “The FTMap Family of Web Servers for Determining and Characterizing Ligand-Binding Hot Spots of Proteins.” *Nature Protocols* 10(5): 733–55. http://www.nature.com/articles/nprot.2015.043.

Kyte, Jack, and Russell F. Doolittle. 1982. “A Simple Method for Displaying the Hydropathic Character of a Protein.” *Journal of Molecular Biology* 157(1): 105–32. https://linkinghub.elsevier.com/retrieve/pii/0022283682905150.

Ngan, Chi-Ho et al. 2012. “FTSite: High Accuracy Detection of Ligand Binding Sites on Unbound Protein Structures.” *Bioinformatics* 28(2): 286–87. https://academic.oup.com/bioinformatics/article-lookup/doi/10.1093/bioinformatics/btr651.

De Oliveira Rodrigues, Thiago Assis, Larissa Fernandes Leijôto, Poliane C. Oliveira Brandão, and Cristiane Neri Nobre. 2015. “Predição de Função de Proteínas Através Da Extração de Características Físico-Químicas.” *Revista de Informática Teórica e Aplicada* 22(1): 29. http://seer.ufrgs.br/index.php/rita/article/view/RITA-VOL22-NR1-29.

Pettersen, Eric F. et al. 2004. “UCSF Chimera?A Visualization System for Exploratory Research and Analysis.” *Journal of Computational Chemistry* 25(13): 1605–12. http://doi.wiley.com/10.1002/jcc.20084.